GEOCHEMICAL EXPLORATION OF GEOTHERMAL PROSPECTS: A CASE STUDY OF MENENGAI, KENYA

Isaack Kanda
Geothermal Development Company Ltd.
P.O. Box 17700-20100, Nakuru
KENYA
ikanda@gdc.co.ke

ABSTRACT

Regional exploration for geothermal resources in Kenya indicates that the Quaternary volcanic complexes of the Kenya rift valley provide the most promising prospects for geothermal exploration. A number of geoscientific studies have been conducted to assess the geothermal potential of this area. This paper reports the results of a survey of fumaroles gas and condensate analysis, alongside CO_2 soil fluxes and concentrations of thoron (Rn_{220}) in soil gases. The procedures employed in the study are divided into: fumarole steam condensate and gas sampling and soil gas sampling to determine mainly the concentrations of carbon dioxide and radon radioactivity. For fumaroles, steam and condensate samples were collected for various analyses. Soil CO_2 concentrations measurements were performed using an Orsat apparatus whereas Rn_{220} soil gas concentrations were measured with a portable radon detector (emanometer). A total of 275 sampling points were measured. The obtained values ranged between zero to 12% of CO_2 in total gas and zero to 6425cpm of Rn_{220}.

The TH_2S geothermometer gave temperatures ranging from 279°C-296°C while TH_2S-CO_2 gave temperatures ranging from 274°C-304°C. The two geothermometers correlate well and from the temperature estimation, it is clear that the reservoir temperatures beneath Menengai caldera are over 270°C. Peak levels of soil CO_2 concentrations and thoron concentrations were identified to be located on major faults and within the caldera floor where hydrothermal fluids are rising and the rocks are highly fractured allowing the release of CO_2 and thoron locally marked by fumaroles. Areas identified with the highest anomalies for CO_2 and thoron soil gas concentrations can be seen in the contour maps presented. The caldera, Molo TVA and also Solai graben are the important geological structures associated with these anomalies.

1. INTRODUCTION

The Menengai Geothermal Prospect is located in the central section of Kenyan Rift Valley, the area north of L. Nakuru and south of Lake Bogoria. The extend of the prospect covers an area of approximately 600km^2 characterized by a complex geological setting with Menengai caldera being notably the major geological feature in the area and is also important for its geothermal potential. Most part of this area, in particular the southern section is discussed in this study.
The general exploration for geothermal resources in Kenya indicates that the Quaternary volcanic complexes of the Kenya rift valley provide the most promising prospects for geothermal exploration,

and as a result, intensive exploration work has focussed on areas with volcanic centres located within the rift valley. Studies show that these volcanic centres have positive indications of geothermal resource that can be commercially exploited. Menengai geothermal area is one of the priority prospects in the current prospects ranking. Eleven locations with fumaroles have been identified in the region (Figure 1).

A number of thermal anomalies and diffuse degassing assessments have been carried out in most of geothermal prospect areas in Kenya, including Menengai. Results for CO_2 and Rn_{220} soil diffuse concentrations have been found to discharge more in areas that coincide with faults. The purpose of this study is to establish the soil gas concentration of CO_2 and Rn_{220} and relate with known geological structures.
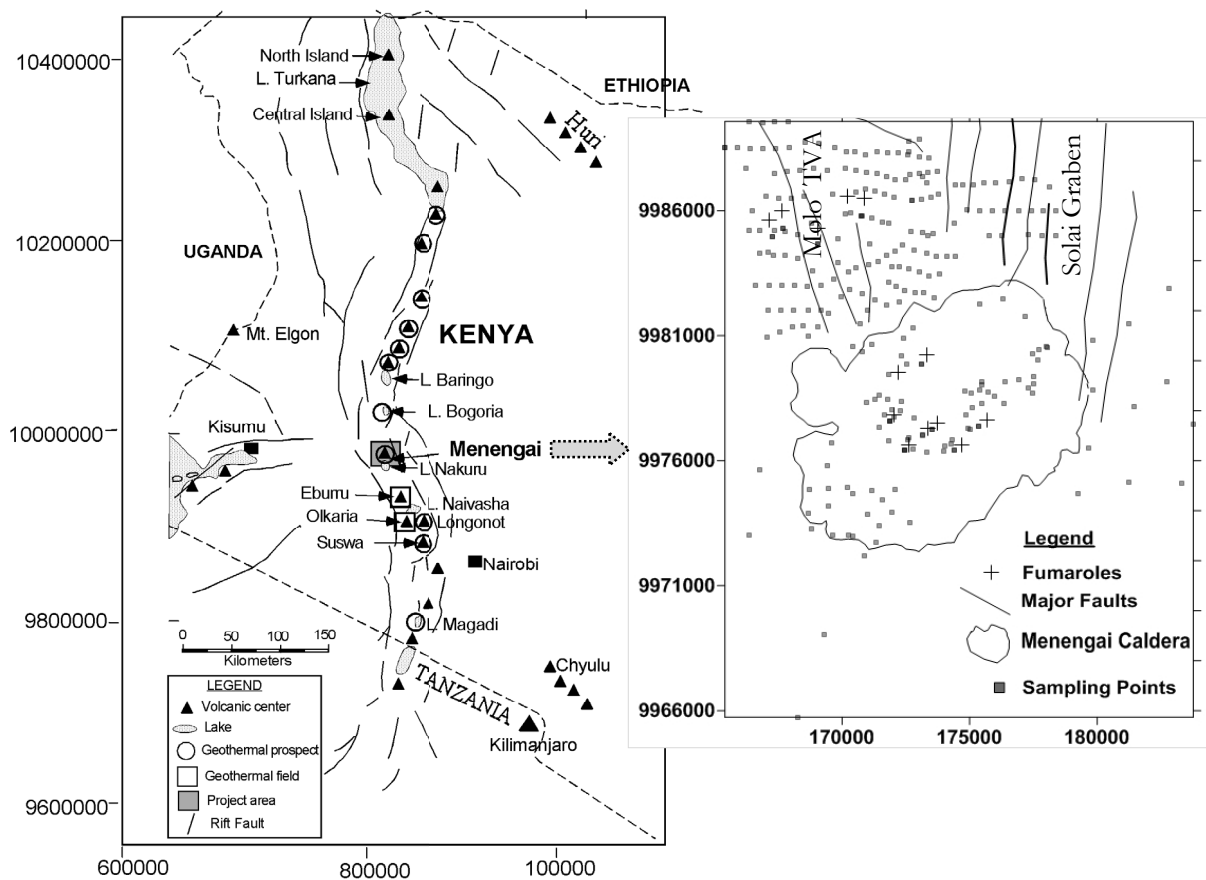

FIGURE 1: Location of Menengai geothermal prospect showing fumaroles, major faults and sampling points

2. GEOLOGICAL AND STRUCTURAL PATTERN

The Kenyan Rift is characterized by extension tectonism where the E-W tensional forces resulted in block faulting (KenGen 2004). This included leant blocks as evident in both the floor and scarps of the rift. The rift trough is truncated by several normal faults, which evidently represent persistent and wide-ranging tectonism under the rift floor. Menengai Geothermal Prospect itself is located within an area characterized by a complex tectonic activity associated with the rift triple junction; the latter being a zone at which the failed rift arm of the Nyanza rift joins the main Kenya rift. Two rift floor tectono-volcanic axes (TVA) that are important in controlling the geothermal system in study area include the Molo and the Solai TVA.

Menengai (Figure 2) has been active from about 0.4 -0.3 Ma B.P (Gislason 1989). The formation of the shield volcano began about 200,000 years ago and was followed by the eruption of two voluminous ash-flow tuffs, each preceded by major pumice falls. More than 70 post-caldera lava flows cover the caldera floor, the youngest of which may be only a few hundred years old. The caldera of Menengai volcano lies immediately north of Lake Nakuru, but ignimbrites and air-fall tuffs from the volcano cover

FIGURE 2: Geological map of Menengai Geothermal Prospect Area (after KenGen 2004)

some 1350 km^2 (Leat & Macdonald 1984) extending into Molo area (Jennings 1971). The volcano is mainly composed of strongly peralkaline, Si-oversaturated trachytes and has had a complex geochemical evolution, resulting from the interplay of magma mixing, crystal fractionation and liquid state differentiation (Leat & Macdonald 1984).
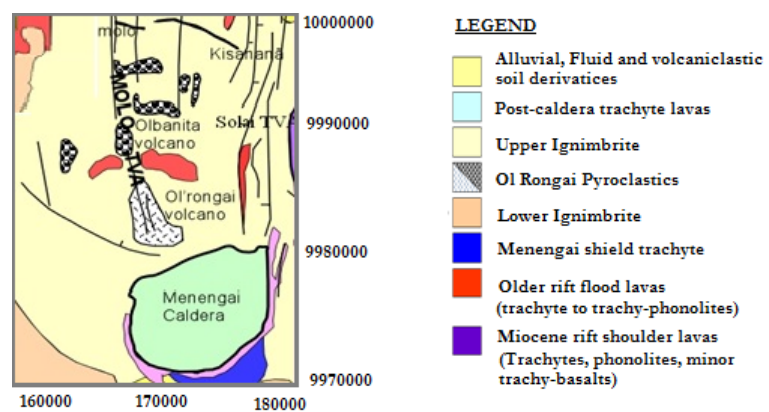
3. METHODOLOGY

The procedures employed in the study are divided into: fumarole steam condensate and gas sampling and soil gas sampling to determine mainly the concentrations of carbon dioxide and radon radioactivity. For fumaroles, steam and condensate samples were collected for various analyses. A portion of the condensate collected was set aside for immediate analysis and measurements of pH, conductivity, TDS, H_2S and CO_2. Electrical conductivity and TDS of the condensate was measured using a portable TDS/conductivity meter and the pH was measured by a pH meter. Zinc acetate was added to another portion of the condensate to fix SO_4^{-2}. Another (untreated) portion was reserved for analysis of chloride (Cl$^-$) and fluorides (F$^-$) in the laboratory.

A different sample was also collected and preserved with concentrated nitric acid for later analysis of metal ions. The analysis of the metals (Na, Ca, K, Mg and Li) was done using the Atomic Absorption Spectrophotometry method and Ion Selective method. The portion for silica (SiO_2) analysis was diluted ten times to avoid polymerization of monomeric silica. The analysis of SiO_2 was done using the UV/VIS spectrophotometry method. Cl$^-$ and F$^-$ were analyzed by the Mohr titration and the ion selective electrode methods for the components respectively. CO_2 and H_2S gases were analyzed using titration methods by using 0.01 M hydrochloric acid (HCl) and 0.01M mercuric acetate, respectively.

The fumarole gases were sampled by directing the steam into two evacuated gas flasks for each fumarole, one at a time, containing 50 ml of 40% NaOH. The acidic gases (CO_2 and H_2S) are absorbed into the NaOH solution giving room in the evacuated flask for the minor none condensable gases usually found in thermal fluids to concentrate to measureable levels. The sample from one of the flask was used for analysis of H_2, CH_4, N_2 and O_2 by Gas Chromatography. From the second flask, CO_2 and H_2S were determined by titrating with HCl and mercuric acetate, respectively, as done for the condensate samples. The water samples from the hot springs and boreholes waters were sampled for analysis of cations and anions. The pH, TDS, Conductivity and sampling temperature were determined in the field.

The CO_2 gas as % of the total gas was measured using the Orsat apparatus. Soil gas samples were obtained using a spike, equipped with a steel outer jacket to penetrate the ground to a depth of 0.7 m. This method of obtaining gases from ground is similar to the one applied for the acquisition of Rn222 radioactivity. The soil gas sample containing radon was pumped into the decay chamber of the

emanometer consisting of a cylindrical copper can, whose walls are coated with zinc sulphide where the radon decays into other radio-nuclides by emitting alpha particles. Three background counts were recorded at two-minute intervals prior to introduction of the sample into the emanometer. An infra-red thermometer was used to take the temperature by directly pointing it into the hole made by the spike and the resultant temperature recorded. Soil gas sampling points ranged from 200m to 2km depending on accessibility, proximity to manifestations and time (see Figure 1).

The study area together with a total of 275 soil gas sampling points is presented in Figure 1. Soil gas survey sampling spacing relied mainly on accessibility of specific targeted points and the ease of getting samples, in particular on the rugged areas. Nonetheless, a random separation of about 300m in average was used. Areas covered by younger lava flow were almost impossible to sample and few samples thus represents such areas, as was seen with lava pond within the caldera. The survey involved measuring of CO_2 and $Rn\text{-}220$ in the soil gas. All the measurements were done at the same point. In addition, soil temperatures were taken using an infra-red thermometer at the point where the soil gas survey was undertaken.

Measurement of CO_2 gas was done by the help of an Orsat apparatus after the soil gas was hand pumped from a depth of 1m below the surface via a hole made using a steel spike with jacket. The Orsat apparatus consist of absorption vessels, which measure about 100mls and contain a 40% KOH solution for absorbing the acidic CO_2. The corresponding volume changes in the absorption vessel represent the corresponding amounts of the gases in volumes given as percent of the total gas as a percentage.

Radon radioactivity levels were measured in the soil gas using a portable radon detector (emanometer). The soil gas was passed into the emanometer by using a hand-operated vacuum pump and $Rn\text{-}220$ readings recorded in counts per minute (cpm). Three background counts were recorded at three-minute interval prior to introduction of sample into the emanometer. Upon introducing the sample, three more readings were taken at one-minute interval to give the total radon counts.

The CO_2 and Rn_{220} obtained in the survey (both 2004 and 2010 sampling programs) were corrected and used to construct concentrations contour maps (Figures 3 to 6). Natural neighbor contouring method was used because it interpolates scattered and irregularly spaced data effectively and hence produces better contours maps from irregularly spaced measurements (Ledoux & Gold 2005).

Early geochemical studies on diffuse soil degassing have been carried out in a number of geothermal areas. CO_2 soil gas investigations similar to the one used in this study have been conducted elsewhere in volcanic areas to examine unexpected rise in CO_2 flux (e.g. Farrar *et al.* 1995; McGee and Gerlach 1998; Gerlach *et al.* 1998), estimate total volcanic flux from volcanic vents and diffuse flank emissions (e.g. Allard *et al.* 1991; Chiodini *et al.* 1996), and to classify tectonic structures related to volcanic degassing (e.g. Giammanco *et al.* 1997; Bergfeld 1998).

4. RESULTS AND DISCUSSIONS

The results of descriptive statistics of CO_2, Rn_{220} and Temperature collected are presented in Table 1. The frequency distributions are described by normal distribution. The range of values for these parameters spans several orders of magnitude.

TABLE 1: Descriptive statistics of CO_2, Thoron and Temperature from 275 sampling points

	N	Range	Minimum	Maximum	Mean	Std. Deviation	Variance	Skewness		Kurtosis	
	Statistic	*Statistic*	*Statistic*	*Statistic*	*Statistic*	*Statistic*	*Statistic*	*Statistic*	*Error*	*Statistic*	*Error*
Rn220	275	6427	0	6427	386	603	363391	5.14	0.15	39.49	0.29
CO2	275	12.30	0.00	12.30	1.12	1.54	2.37	5.12	0.15	30.81	0.29
Temp	275	55.90	21.20	77.10	28.70	6.99	211.52	0.05	0.15	0.62	0.29

4.1 Soil temperature measurements

The mapping of temperature variations at or below the earth's surface is an essential geothermal exploration instrument. The spatial variation of soil temperature is illustrated in Figure 3. Quite a number of anomalies can be identified in relation to the major structural setting. And as indicted by results, a higher temperature anomaly in the caldera is evident around the fumaroles with the highest fumaroles temperature of 88°C. Similar to other soil surveys, soil temperature results in the caldera is mainly affected by the lava that covers the caldera floor and apart from the areas where the lava did not cover. The areas to the North outside the caldera gave an anomaly confirming the geothermal potential of the area coinciding with two major faults trending NW-SW.

4.2 Diffuse degassing measurements

The term volcanic gas defines a gas exsolved from a magmatic source of an active volcano whereas hydrothermal gas defines a gas exsolved from the envelope of hot water that surrounds the magmatic environment. Volcanic gases have composition different from the hydrothermal gases, the first is richest in SO_2 and the second in H_2S (Giggenbach 1996). CO_2 occurs in both magmatic and hydrothermal gases and is the most abundant gas after water vapor. The deep-seated faults in the crust tap magmatic CO_2, which is transmitted to the surface where it is naturally lost through the soil. Carbon dioxide (CO_2) of magmatic origin is normally channeled through deep-seated tectonic structures close to the surface of the earth and then seeps out of the ground through the soil. However, dealing with CO_2 anomalies especially in the Rift Valley ought to be treated with caution owing to the availability of localized sources of this gas as suggested by Darling *et al.* (1995). CO_2 may also originate from other sources like organic matter, which are likely to give false impressions of a geothermal source.

Thoron gas (Rn_{220}) is a short lived isotope of radon produced by the thorium (Th_{232}) decay series with a half-life of 55 seconds (Lopez *et al.* 2004). Due to its short half-life, thoron's transportation is limited to a few centimeters either by diffusive or convective flows, as compared to Rn_{222} (t ½ = 3.8 days) (Hutter 1993). As a result, the high concentrations of thoron are more likely to be due to convective movement of gases rather than diffusive processes and therefore it is difficult to achieve an exact quantitative measurement of its concentration. If we measure the disintegration of thoron, it shows a decrease during the first three minutes after collection of the sample, as opposed to the radon that presents a half-life of almost 4 days (Magana *et al.* 2002). High thoron values could be suggestive of enhanced permeability, as it may as well depend on other factors such as the degree of rock fracture and the ability of groundwater to circulate and remove thoron.

The CO_2 gas concentrations are plotted in Figure 4 while the results of radon emanations were recorded in counts per minute (cpm) for Rn_{-220} and plotted in Figure 5. To reduce interferences between CO_2 and Radon sources a ratio of Rn_{-220}/CO_2 have been plotted in Figure 6.

4.2.1 CO_2 concentrations

The concentration of CO_2 in the soil gas in the surveyed area is given as a percentage of the total gas in the soil. The degassing of CO_2 through the soil in the prospect area is considered to be mainly
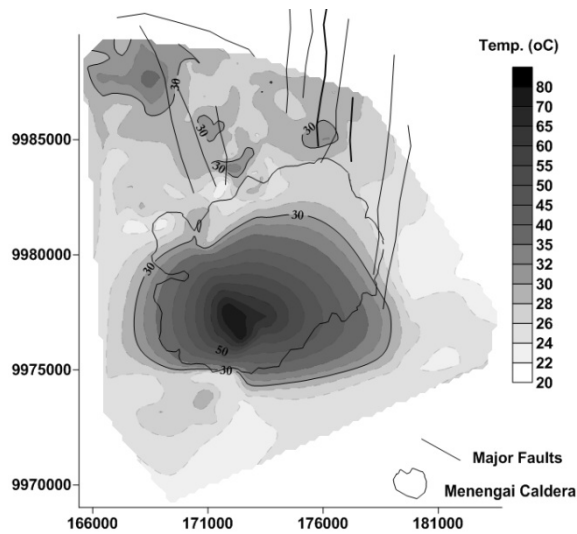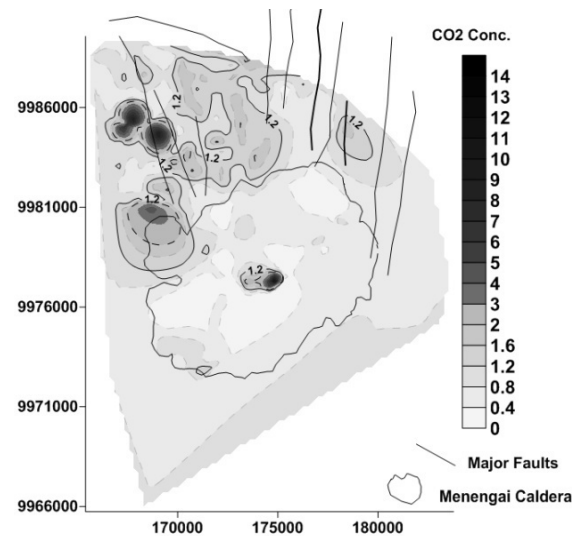
FIGURE 3: Temperature distribution in $^{\circ}$C

FIGURE 4: CO_2 conc. distributions

supplied by two sources, the one of volcanic origin emanating from deep environment and a shallow one that result from organic activity. In this study, high CO_2 values (>2.5%) are found at a belt running in a NW-SE while other areas exhibit low values (<1 %). These areas coincide with the Molo Tectono-Volcanic Axis (Molo TVA), deep seated faults and the eruption centers in the prospect area which indicate that the source could be from a magmatic body. Highest CO_2 concentration in the soil gas was observed around Ol'Rongai Hill (located along Molo TVA) and the contiguous fumaroles with CO_2>10% which could be indicative of good permeability in the area.

The central part of the caldera around the fumaroles, as well, displays relatively high values of CO_2 (>2.8%). There are also few highs of CO_2>5 % in the western part of the caldera. The presence of thick young lava that covers most parts of the caldera interfere with the movement of CO_2 to the surface and therefore makes sampling in these parts extremely difficult, and is also noticeable in the contouring of the CO_2 distribution as shown in Figure 4. Care ought to be taken while correlating thermal and diffuse degassing anomaly with subsurface permeability.   This is because the cap of young lava that covers most part of the caldera might be directing the anomaly laterally beneath the lava bed and hence giving misleading impression as a result.

4.2.2 Thoron concentrations

From the results of the absolute values of Rn_{-220}, north-western parts of the surveyed area show the highest concentrations (Figure 5). In addition, a more pronounced anomaly is evident in central part of the caldera in the areas adjoining fumaroles following similar pattern to the one revealed by CO_2 distributions. However, a mild rise in thoron values is seen in the eastern flank touching Solai Graben.

4.2.3 Thoron-CO_2 ratios

The ratio of the Rn_{220}/CO_2 gases would be a good indicator of the magmatic source of the gases since the ratio is not expected to change if they are from the same source (see Figure 6). High values of these ratios are found towards the north, north-western to the north eastern parts outside of the caldera wall with two anomalous areas at the fumaroles in Ol'Rongai area. A mantle source of CO_2 as suggested by Darling et al. (1995) is a possibility of the source of this gas due to intense faulting in the area, and these faults around Ol'Rongai are of great importance in localizing degassing of CO_2 and Rn_{-220} as well thermal manifestation anomalies. If a mantle source is inferred due to intense faulting, then the faults should be deep seated. These areas apparently coincide with high CO_2 and high Rn-220 absolute values.
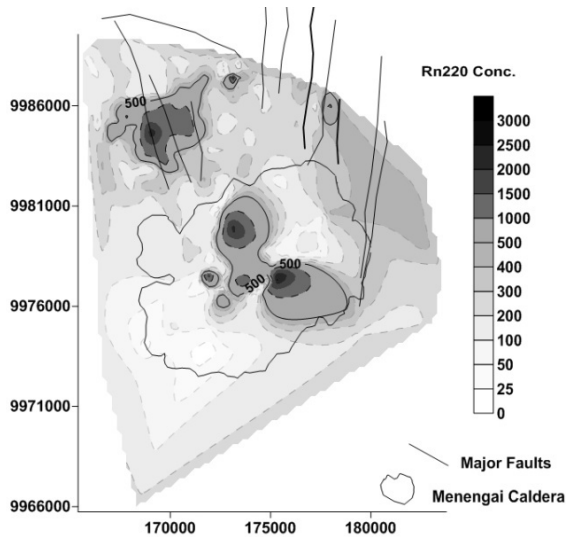
FIGURE 5: Rn_{220} conc. distributions
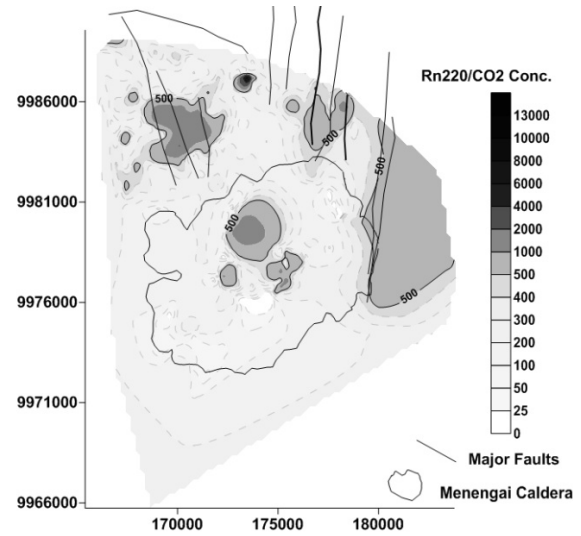
FIGURE 6: Rn_{220}/CO_2 conc. distributions

The western part of the surveyed area, which shows high absolute values of CO_2, gives low value of this ratio. This is an indication of a source other than the one of magmatic origin. This coincides with an agriculture farm and consequently the CO_2 anomaly in this area is considered to emanate from organic source, as a result. Nonetheless, a higher ratio of these gases is seen within and to the east of the caldera.

4.3 Fumarole gas analysis

Samples collected during the infill survey show atmospheric air contamination as they contain high values of nitrogen and oxygen. Fumarole temperature measurements differ significantly for the CO_2 and H_2S with CO_2 temperatures being unrealistically high.

4.4 Fumarole steam condensates

The chemical constituents analysed in the steam condensates are those which can be considered to be volatile enough to partition into the steam phase upon phase separation in a boiling system as is expected in an aquifer producing steam. Such elements include the soluble gaseous compounds such as CO_2, H_2S, F^-, and B, which are present in the geothermal steam. In addition, the concentration of other non-volatile elements like Cl^-, SiO_2 and SO_4^{-2} were determined. The pH, TDS and the electrical conductivity were also measured in the steam condensate samples.

TABLE 2: Rn-222 radioactivity and CO_2 concentration in fumarole steam

Fumarole No.	Location		Elevation (m)	CO_2 (%) vol.	Temp °C	Rn-222 (cpm)	Rn/CO$_2$ ratio
	Eastings	Northings					
MF-1	172400	9975900	2160	15.1	60.0	1650	109.3
MF-2	175324	9977356	1992	25.6	94.0	12194	476.4
MF-3	171868	9977563	2081	16.7	77.1	2200	131.7
MF-4	169080	9984679	2016	48.2	81.2	3700	76.76
MF-5	167712	9985324	1896	43.8	86.1	2890	66.0
MF-6	173208	9979555	1908	32.6	84.6	16848	516.8
MF-7	173682	9977020	2106	18.3	73.5	1600	87.4
MF-8	174485	9976115	2098	24.6	90.1	1580	64.2

TABLE 3: Fumarole steam condensate analysis from Menengai geothermal prospect

Fumarole No.	Fumarole Location		Fumarole Temp (°C)	pH	Cond (µS)	TDS (ppm)	Hg (mg/m³)	Condensate (ppm)										
	Easting's	Northing's						CO_2	H_2S	B	Ca	Cl	F	K	Li	Mg	SiO_2	SO_4
MF-1	173170	9977023	62	6.7	4.0	2.0	0.000	109.3	0.3	0.2	5.7	0.2	0.2	0.8	nil	0.1	12.4	3.8
MF-2	175353	9977375	88	6.8	14.0	7.0	0.024	41.1	0.1	0.1	5.2	2.5	0.2	0.5	nil	0.2	0.2	4.5
MF-3	171876	9977567	85	6.7	0.0	0.0	0.140	39.6	0.4	0.1	5.8	1.6	0.2	2.2	nil	0.8	0.4	10.3
MF-6	173112	9979852	75	6.5	23.0	11.0	0.013	54.1	0.3	0.4	3.3	1.7	1.3	0.0	nil	0.0	0.9	3.9
MF-7	173520	9977240	88	6.1	2.0	0.0	0.003	35.6	0.3	0.3	2.8	1.3	0.1	0.9	nil	0.0	0.3	9.6
MF-8	174395	9976411	88	6.0	3.0	1.0	0.003	33.9	0.1	0.2	2.8	2.0	0.3	0.9	nil	0.2	0.3	6.7
MF-9	172441	9976400	70	6.2	4.0	2.0	0.000	37.4	0.1	0.2	5.7	2.0	0.7	2.3	nil	0.4	0.4	0.2

5. DISCUSSIONS AND CONCLUSIONS

The fumarole steam was analysed for the major gases associated with geothermal activity (CO_2, H_2S, H_2, CH_4 and N_2) and the results indicate no hydrogen and methane for all the samples obtained. Most of these fumaroles were issuing at extremely low pressures and it was quite difficult to obtain condensate samples from the fumaroles. From the analytical results obtained, such weak fumaroles have compositions indicating high air/steam ratios. Such high ratios are indicative of shallow surface waters locally mixing with steam and hence the bulk composition of the gases is composed of atmospheric air.

The gas contents of fluids present in areas of high permeability and close to a hot geothermal fluid upflow are expected to be of high concentrations especially with regards to the reactive gases like CO_2, H_2S and H_2. Hydrogen and methane are lacking but high CO_2 and H_2S occurs in fumaroles MF2 and MF6. When the fluid travels for long distances there is a tendency for it to be depleted of these gases through possible reactions between the gases and the minerals forming the reservoir rocks. On the other hand, the concentration of N_2 in the fumarole steam could be an indicator of admixture with gas originating from the atmosphere. This could be taken to imply mixing of shallow ground waters with deep geothermal fluids. The N_2 gas is considered largely to be derived from air and then introduced into the geothermal system. There are possibilities of N_2 accumulating in the rocks from organic life.

Temperatures were calculated for five fumaroles sampled. The TH_2S geothermometer gave temperatures ranging from 279°C-296°C while TH_2S-CO_2 gave temperatures ranging from 274°C-304°C. The two geothermometers correlate well and from the temperature estimation, it is clear that the reservoir temperatures beneath Menengai caldera are over 270°C.

Fumarole condensate samples were analysed for pH, TDS, CO_2, H_2S, Cl^-, F^-, B, SO_4^{-2} and the electrical conductivity. All the condensates gave pH values ranging between 6 at MF-8 and 7.5 at MF-2 measured at 20°C. Low pH values imply the fluids contain high concentrations of acid gases, which form the acidic condensed water. Most of the acidic emanations are mainly magmatic with large amounts of volatile components such as H_2O,

HCl, SO_2, H_2S, CO_2 and H_2. However, chemical properties of magmatic emanations collected on the surface are expected to be different from those under the ground on account of severe distillation on the surface caused by depression of pressures and temperatures.

Volatile chemical constituents dissolved in the deep water would be transported to the surface with steam from greater depth through vaporization. High volatility elements like F^-, B, NH_3, arsenic (As) and mercury (Hg) would therefore be expected to dominate in the steam composition in addition to the geothermal related gaseous elements (CO_2, H_2S and H_2). High concentration of volatiles in a steam condensate would be proportional to strength of the discharge and temperatures of the steam source.

All the condensate samples gave F^- values ranging from <0.1-1.3 ppm while the B values range from 0.1-0.4ppm for fumaroles MF-2 and MF-6 respectively. The relatively high F^- content in the steam condensate may indicate deep crustal water circulation while at the same time the relatively high B values in the condensate may indicate high formation temperatures. Boron is considered a mobile component since it does not take part in rock forming reactions and its concentration in the geothermal fluids is controlled by the leaching rate from the reservoir rocks. At high temperatures (>250°C) boron is expected to partition into the steam phase and if boiling is occurring in the reservoir, then the temperatures should be more than 250°C. The difference in boron concentration of different fumarole steam condensates can partly be due to the compositions of the source rocks.

The Cl^- content of the condensate samples from fumaroles MF-4 and MF-8 ranged from 15.6–34.1 ppm respectively. Very high Cl^- values in a steam condensate would represent a water dominated system while extremely low values would be expected to originate from a vapour dominated system since chlorides are not known to partition into steam phase at any temperatures.

Despite the erratic distribution of sampling points, the results from acquired data can be used to make some conclusions relative to the objective. The fumaroles show close relations with geologic structures, which provides means of access for hydrothermal fluids to reach the surface. In the same way, most of the gas anomalies are located in fault zones. CO_2 and Rn_{220} emanations from the presently quiescent faults in Menengai were measured to be higher than background values.

The two fault-lines at Ol'Rongai are considered in this study to be of great importance in geothermal exploration and any future development as it reflects intensity of subsurface permeability in the area, and enhances the confidence to invest. The caldera itself as a geological structure displays a positive evidence of the existence of geothermal resource, with its thermal anomalies that coincides with CO_2 and thoron anomalies. Nonetheless, the picture portrayed by the contours within the caldera is hereby treated with caution as the pond of new lava spread across most part of the floor greatly influenced sampling spaces, and possibility of lateral flow of thermal fluids and diffuse gases at the upper zones restricted by the lava cap cannot be negated.

Generally, CO_2 concentrations are structurally controlled but may have been modified by changes in land use. As seen from the findings, the study of soil CO_2 and Rn_{220} composition as proved to be important geochemical method to identify vertical zones of high permeability. The employment of these methods in other geothermal fields could give important and relatively cheap information for field utilization and development.

REFERENCES

Allard, P., Carbonnelle, J., Dajlevic D., le Bronec, J., Morel, P., Robe, M.C., Maurenas, J.M., Faivre-Pierret, R., Martin, D., Sabroux, J.C., and Zettwoog, P., 1991: *Eruptive and diffuse emissions of CO_2 from Mount Etna. Nature, 351*, 387–391.

Bergfeld, D., Goff, F., Janik, C.K., and Johnson, S.D., 1998: CO_2 Flux Measurements across Portions of the Dixie Valley Geothermal System, Nevada. *Geothermal Resources Council Transactions, 22*, 20-23.

Chiodini G., Frondini F. & Raco, B., 1996: Diffuse emission of CO2 from the Fossa crater, Vulcano Island _Italy. *Bull. Volcanol., 58*, 41–50.

Darling, W.G., Griesshaber, E., Andrews, J.N., Armannsson, H., and O'Nions, R.K., 1995: The origin of hydrothermal and other gases in the Kenyan Rift Valley. *Geochim. Cosmochim. Acta, 59*, 2501-2512.

Farrar, C.D., Sorey, M.L., Evans, W.C., Howle, J.F., Ken B.D., Kennedy, B.M., King, C.Y., and Southon, J.R., 1995: Forest-killing diffuse C02 emission at Mammoth Mountain as a sign of magmatic unrest. *Nature, 376*, 675-678.

Gerlach, T.M., Doukas, M.P., McGee, K.A., and Kessler, R., 1998: Three-year decline of magmatic CO_2 emissions from soils of a Mammoth Mountain tree kill: Horseshoe Lake, CA, 1995-1997. *Geophy. Res. Lett., 25*, 1947-1950.

Giammanco, S., Gurrieri, S., and Valenza, M., 1997: Soil CO2 degassing along tectonic structures of Mount Etna (Sicily): the Pernicana fault. *Appl. Geochem., 12*, 429–436.

Gislason, G., 1989: Terminal Report of Exploration for geothermal energy KEN/82/002, *United Nations* DTCD.

Hutter, A. R., 1993: Thoron/radon (220Rn/222Rn) ratios as indicators of soil gas transport: *Geological Society of America Abstracts with Programs, A 195*.

KenGen, 2004: *Menengai volcano: investigations for its geothermal potential. A Geothermal Resource Assessment (GRA) project*. Internal Report.

Leat, P.T., and Macdonald, R., 1984: Geochemical Evolution of the Menengai Caldera Volcano, Kenya. U.S Geology Survey. *Journal of Geophysical Research, 89,* 8571-8592.

Ledoux, H. & Gold, H., 2005: An Efficient Natural Neighbour Interpolation Algorithm for Geoscientific Modelling. In *Developments of Spatial Data Handling by Peter F Fisher. 11th International Sysmposium on Spatial Data Handling*, 97-109.

Lopez, D.L., Ransom, L., Perez, N., Hernandez, P., and Monterrosa, J., 2004: Dynamics of diffuse degassing at Ilopango Caldera, El Salvador. In: Rose, W.I., Bommer, J.J., López, D.L., Carr, M.J., and Major, J.J. (eds): Natural Hazards in El Salvador. *Geological Society of America Special Paper, 375,* 191-202.

Magaña, M., Lopez, D., Tenorio, J. & Matus, A., 2002: Radon and Carbon Dioxide Soil Degassing at Ahuachapan Geothermal Field, El Salvador. *Geothermal Resources Council Transactions, 26*, 341-344.

McGee, K.A., and Gerlach, T.M., 1998: Annual cycle of magmatic CO_2 at Mammoth Mountain, California: Implications for soil acidification. *Geology, 26*, 463-466.